Band-Shape Analysis of Delayed Slow-Passage ODMR in the Photoexcited Triplet State of Tryptophan

Andrzej Ozarowski and August H. Maki*

Department of Chemistry, University of California Davis, Davis, California 95616

Received: September 29, 1999; In Final Form: November 24, 1999

Delayed slow passage optically detected magnetic resonance (ODMR) band shapes of the triplet state of tryptophan, lysyl-tryptophanyl-lysine, *N*-acetyl tryptophanamide, and ribonuclease T1 from *A. oryzae* (RNaseT1) in low-temperature aqueous glass are analyzed using data obtained from independent microwave-induced delayed phosphorescence (MIDP) measurements as fixed input parameters. This method which uses only the band center frequency, Gaussian width, overall amplitude, and baseline position as variables is compared with a previously employed empirical analysis (Wu, J. Q.; Ozarowski, A.; Davis, S. K.; Maki, A. H. *J. Phys. Chem.* **1996**, *100*, 11496) that requires many more variables. Comparable quality of fit is found for the new, more rigorous method for each band except for the $T_x \leftrightarrow T_z$ (D−E) ODMR transition which (with the exception of RNaseT1) deviates systematically when using the fixed kinetic parameters. The quality of fit of this band becomes comparable to that of the multiparameter empirical method upon introduction of dispersion in k_x, which assumes values between −1 and −2 s^{-1}/GHz. The sign and magnitude of this dispersion are consistent with previous kinetic data. Band centers and widths are altered only slightly from those obtained by the earlier empirical analysis.

Introduction

Magnetic resonance line shapes are influenced by rapid passage effects when relaxation times are comparable to or longer than the passage time through the resonance line. In EPR spectroscopy of an isolated electronic state, spin−lattice relaxation (SLR) alone controls the dynamics of rapid passage effects. In the case of a photoexcited triplet state, however, passage effects on line shapes can be influenced not only by SLR but also by the decay rates of the sublevels to the ground state, and by their populating rates if EPR is measured during optical pumping.

Optical detection of magnetic resonance (ODMR)[1] in the photoexcited triplet state normally is carried out at cryogenic temperatures below 4 K in order to reduce SLR rates to values comparable to or below the sublevel decay rates to the ground state. The triplet sublevel populations then can be maintained far from thermal equilibrium, thus enhancing ODMR signal intensity. Under these conditions, the ODMR band shape will be influenced, in general, by both SLR kinetics and the sublevel populating/depopulating kinetics.

ODMR bandwidths in disordered solids are frequently on the order of 100 MHz as a result of random solute−solvent interactions;[1] microwave hole-burning measurements,[2−4] on the other hand, suggest that the homogeneous line width is on the order of 1 MHz. In the approximation that the inhomogeneous band is composed of a distribution of isolated spin packets of homogeneous width $\delta\nu \sim 1$ MHz, the slow-passage condition

$$\delta\nu/(\mathrm{d}\nu/\mathrm{d}t) > \tau \qquad (1)$$

requires $\mathrm{d}\nu/\mathrm{d}t < 1$ MHz/s if the relaxation time, τ, is the order of 1 s, as is typical for aromatic $^3(\pi,\pi^*)$ states. Microwave sweep rates employed in ODMR spectroscopy in disordered solids are typically on the order of 100 MHz/s. Thus, under these conditions the ODMR band shape can be approximated as a *superposition of rapid passage transients* produced by the distribution of spin packets that constitute the band. The optical response of the αth spin packet to rapid passage connecting sublevels T_i and T_j ($i, j = x, y, z$) is given by eq 2 under conditions of weak optical pumping (neglect of populating rate constants) and negligible SLR:[5]

$$I_\alpha^{ij}(t) = CG_\alpha[k_i^{\mathrm{r}} \exp(-k_i t) - k_j^{\mathrm{r}} \exp(-k_j t)] \qquad (2)$$

I_α is the phosphorescence intensity and G_α is the population of the αth spin packet, k_i and k_i^{r} are overall and radiative decay constants of T_i, respectively, and C depends on the experimental arrangement and the spin alignment. In previous work[6,7] we have adopted eq 2 as an approximation and have used a nonlinear least-squares treatment to fit the experimental band shape to a distribution of G_α, assumed to be Gaussian. The best fit band-shape parameters, ν_0 and $\nu_{1/2}$, the peak frequency and the half-width at half-height of the Gaussian band, respectively, were found to be remarkably invariant over a wide range of microwave sweep rates, lending confidence to this model. This empirical model succeeded for "slow-passage" ODMR during both continuous optical pumping[6] where C is constant and during decay of the triplet state (delayed ODMR)[7] when it changes with time.

The best-fit values obtained for the k's and relative k^{r}'s[6,7] are not true kinetic parameters, however, since SLR was not negligible under the experimental conditions nor were the populating rates negligible during optical pumping. In delayed ODMR, eq 2 is incorrect in principle, since the transient response to fast passage consists of the superposition of *three* exponential components, given by the eigenvalues of the rate constant matrix, rather than the biexponential form of eq 2. Also, the time dependence of C must be expressed in terms of the

* To whom correspondence should be addressed.

10.1021/jp993500r CCC: $19.00
Published on Web 01/14/2000

same three eigenvalues. It is now possible, using global analysis[8] of microwave-induced delayed phosphorescence (MIDP)[9] data sets, to obtain both the decay rate constants, k_i, and the SLR rate constants, W_{ij}, independently. From these and the relative initial sublevel populations, also found by the analysis, the eigenvalues and eigenvectors of the rate constant matrix can be calculated. The relative k^r's are obtained as well, so that phosphorescence intensities can be related to the sublevel populations. Thus, global MIDP analysis yields the information that is sufficient to calculate rigorously the band shape by least-squares analysis of the delayed ODMR response using independently determined kinetic data, initial populations, and radiative parameters as input parameters.

There is a complication that must be considered when applying kinetic data to the analysis of ODMR band shapes of photoexcited triplet states in disordered solids. We have found in previous ODMR studies[10,11] that in disordered solids, SLR exhibits dispersion within the triplet state population whereas in crystalline samples no dispersion is evident. For the triplet state of tryptophan in disordered (glass) media, which is the subject of the current work, we found that the distribution of SLR appears bimodal. At 1.2 K, one subpopulation that exhibits slow SLR, $W_{ij} < k_i$, is responsible for the ODMR responses, while the remaining subpopulation is characterized by rapid SLR, $W_{ij} > k_i$, and is ODMR silent because it lacks significant spin alignment. Fortunately, we can find no subpopulation with intermediate SLR ($W_{ij} \sim k_i$), as kinetic analysis of ODMR responses would not be feasible if such triplet states were present in noticeable amounts.

In this paper, several delayed ODMR data sets are analyzed both by the earlier algorithm that employs initial populations and empirical kinetic and radiative parameters as variables[7] and by use of fixed parameters obtained from global analysis of MIDP as input data. Comparison of these methods suggests that for tryptophan in disordered solids the value of k_x varies with microwave frequency within the D−E ($T_x \leftrightarrow T_z$) band and possibly in the 2E ($T_y \leftrightarrow T_x$) band. Assuming a linear dispersion of k_x within these bands yields a quality of fit comparable to that produced by the empirical method.

Experimental Section

The systems studied were the amino acid tryptophan, the nonpolar analogue, *N*-acetyltryptophanamide (NATA), the tripeptide lysyl-tryptophanyl-lysine (KWK), and the enzyme ribonuclease T1 from *Aspergillus oryzae* (RNase T1) that contains a single interior tryptophan residue that is not solvent-exposed. Samples were dissolved to 0.2−0.4 mM concentration in 10 mM pH 7 phosphate buffer containing 40 vol % ethylene glycol. This solvent composition forms a clear glass on cooling and exhibits a maximum in the tryptophan population with slow SLR (ca. 70%), and thus has the maximum ODMR signal intensity.[10] Samples, contained in 1 mm Suprasil tubes were immersed in liquid He and maintained at 1.2 K by pumping. Samples were excited by a 100 W mercury arc lamp at 297 or 302 nm, selected by a monochromator set at 16 nm band-pass. Phosphorescence was monitored at the 0,0-band peak through a monochromator with 3.2 nm band-pass using photon counting. Details of the ODMR spectrometer have been reported previously.[6,8] All measurements were carried out in zero applied magnetic field and data were accumulated in a 1024-channel multichannel analyzer (MCA). MIDP data were collected and analyzed globally as described previously.[8] Delayed slow-passage signals were obtained by optically exciting the sample for 15 s and monitoring the phosphorescence for ca. 45 s following the closing of a shutter in the excitation path. The microwave frequency was swept slowly through a resonance band after a delay following the closing of the shutter. The incident power level was set at ca. 5 mW. Typical conditions were delay time of 0−15 s and sweep rate of 30 MHz/s. MIDP data were obtained for similar shutter timing conditions, but the microwave frequency was swept through the band at 12 GHz/s so that saturation of a pair of sublevels occurred within 1−2 channels of the MCA. A corresponding free decay curve was recorded for each set of timing conditions and subtracted from the ODMR data set to produce a difference spectrum for analysis. Electron−electron double resonance (EEDOR) was used occasionally to enhance the D + E transition by saturating the 2E band. Saturation was accomplished by a second microwave source whose frequency was modulated at 100 Hz throughout the 2E band.

Theory

At temperatures near 1.2 K where SLR is largely quenched, the phosphorescence of tryptophan decays nonexponentially after optical pumping is terminated. In the absence of microwave-induced transitions, the triplet state decay is described by the system of three coupled equations

$$\frac{dn_i}{dt} = -(k_i + W_{ij} + W_{ik})n_i + W_{ji}n_j + W_{ki}n_k \qquad (3)$$

where i, j, and k run over the triplet state sublevels, x, y, and z, and n_i is the momentary population of sublevel T_i. The solutions of eqs 3 are of the form[12]

$$n_i(t) = \sum_{n=1}^{3} c_{in} \exp(-\rho_n t) \qquad (4)$$

Each sublevel decays as a combination of three single-exponential components with rate constants equal to ρ_n, where $-\rho_n$ are the eigenvalues of the rate constant matrix **R**.[8,12] The weighting factors, c_{in}, are elements of the ith eigenvector of **R** and depend on the initial populations. The relative initial populations and the rate constants that determine **R** are found by the global analysis of MIDP,[8] allowing calculation of $n_i(t)$. The approximation $W_{ij} = W_{ji}$ is justified in this analysis since the zero-field splitting energies ($\sim$0.1 cm^{-1}) are small compared with thermal energy ($\sim$0.83 cm^{-1}). The light intensity emitted by sublevel T_i is proportional to $n_i(t)k_i^r$. The overall light intensity of a spin packet α observed during undisturbed decay is

$$I_\alpha(t) = A\sum_i \sum_{n=1}^{3} c_{in} k_i^r \exp(-\rho_n t) \qquad (5)$$

where A depends on experimental conditions and closing of the excitation shutter occurs at $t = 0$.

At time t_0^α during the decay the resonance frequency of spin packet α is reached and the populations of a pair of triplet sublevels of that spin packet are equalized. This produces a change in the coefficients c_{in} but does not affect the eigenvalues. We have shown previously[10,11] that under our experimental conditions the spin packet populations of tryptophan are equalized but not inverted by fast passage. We may confidently assume, therefore, that at the same microwave power level the spin packet populations also are saturated under the slower sweep conditions employed in the delayed ODMR experiment. Some time ago, Hoff and Cornelissen[13] showed that care must

be employed to ensure complete saturation of the spin population of a randomly oriented sample, since the microwave field is polarized and the sample will contain molecules with unfavorable orientations. Such problems arose in bacteriochlorophyll whose triplet state decay constants are more than a factor of 10^4 larger than those of tryptophan. Thus, saturation of the tryptophan spins would require ca. 80 dB less microwave power than those of bacteriochlorophyll.

The difference between phosphorescence intensity after the fast passage at $t = t_0^{\alpha}$ and the intensity during the natural free decay is

$$\Delta I_{\alpha}(t) = A\sum_i k_i^{r} \sum_{n=1}^{3} \exp(-\rho_n t)[c_{in}^{*} \exp(\rho_n t_0^{\alpha}) - c_{in}] \quad (6)$$

where c_{in}^{*} are the eigenvector elements modified by the fast passage, and $t \geq t_0^{\alpha}$. For $t < t_0^{\alpha}$, $\Delta I_{\alpha}(t) = 0$. If $G(\nu_{\alpha})$ is the population of spin packet α, we have for the overall response,

$$\Delta I(t) = A\sum_{\alpha=1} G(\nu_{\alpha}) \sum_i k_i^{r} \sum_{n=1}^{3} \exp(-\rho_n t)[c_{in}^{*} \exp(\rho_n t_0^{\alpha}) - c_{in}] \quad (7)$$

Note that in eq 7 the same set of c and ρ values is assumed for each spin packet. The calculated response, eq 7, is equivalent to the summation of MIDP responses of individual spin packets[8] weighted by $G(\nu)$ which we will assume has a Gaussian form.

Analysis

The kinetic parameters were taken from global analysis of MIDP data;[8] they were assumed initially to be the same for each spin packet and were not varied in the least-squares procedure. In the fitting of the slow passage spectra, the width of a spin packet was assumed to be equal to the channel width of the MCA which is the same order as the homogeneous line width. We have shown earlier[6] that the spin packet width is not critical for the analysis as long as it is negligible compared with the bandwidth. The variable parameters in the analysis are limited to the center frequency and width of the distribution $G(\nu)$, the overall signal amplitude, and baseline level. A least-squares fitting program was written in C++ for Windows 95/98 that uses the Simplex method. The nature of the problem makes the implementation of more sophisticated algorithms, such as Marquardt−Levenberg, difficult. The necessity of calculating numerically derivatives of the spectrum with respect to parameters in the latter method offsets its faster convergence in comparison with Simplex. We have no analytical formulas for the derivatives since the function to be fitted is given in a very convoluted way. Simplex calculations on a Pentium II 450 MHz computer took in most cases a few hundred iterations over several minutes. The method also proved to be suitable for simulation of EEDOR spectra. Saturation of a pair of sublevels was simulated by assuming very rapid SLR between them.

Quality of fit was judged by a normalized value of χ^2, defined by

$$\chi^2 = \chi^2(\text{MIDP})/\chi^2(\text{empirical}) \quad (8)$$

where χ^2 (empirical) was obtained from the fitting using the earlier empirical method.[7] Due to the large number of adjustable parameters (and the essentially correct nature of the fitting function) the empirical method produces an almost perfect fit even though the resulting kinetic and radiative parameters are not interpretable. One might be tempted to normalize χ^2(MIDP) by χ^2(free decay) obtained from fitting the free decay to a superposition of four exponential decays instead of χ^2(empirical) as this could represent the pure noise. The rationale for the use of a four-exponential fit for the free decay is based on previous work[10,11] in which the triplet states in a glass sample could be divided bimodally into a slowly relaxing population and a residual population in which SLR is dominant. SLR in this latter population is induced by interactions with disorder modes of the glass matrix.[14,15] Each population in this model decays as the superposition of three exponential components, but two that originate from the rapidly relaxing population have very small amplitude, decay rapidly, and do not contribute to the analyzed portion of the free decay. Apparently this bimodal model is somewhat oversimplified since the four-exponential fitting function yields a small systematic error when fitted to the decay. That error source is not present in the data set because the latter is obtained by subtracting the free decay from the delayed ODMR spectrum. In every case, we find that χ^2(empirical) < χ^2(free decay).

In some spectra it was noted that the predetermined input parameters produced a significantly poorer quality of fit than was obtained by the empirical procedure[7] and it could not be improved without changing kinetic parameters. Comparison of responses observed with increasing and decreasing microwave frequency suggested that the fitting could be improved by allowing k_x to vary with microwave frequency over the distribution $G(\nu)$, while leaving its mean value equal to that obtained from MIDP. Calculations that include dispersion in k_x required the evaluation of eigenvalues and eigenvectors for each spin packet and resulted in a substantial increase in computation time.

Results

A representative delayed slow passage ODMR spectrum of the D−E transition of NATA with increasing microwave frequency is presented in Figure 1. The calculated minimum least-squares response using fixed parameters from MIDP is superimposed. The residual is presented in a separate panel. A new minimum least-squares spectrum was calculated with the introduction of an added variable, $dk_x/d(D-E)$, maintaining $\langle k_x \rangle_{av}$ at its MIDP value. The residuals for this new fitting also are shown in Figure 1 (circles). The value of χ^2 is reduced by a factor of 6.1 (increasing frequency) by a best-fit value of −1.2 s^{-1}/GHz. The delayed slow-passage D−E band of KWK with increasing microwave frequency is shown in Figure 2A. Superimposed is the best-fit spectrum based on fixed MIDP parameters. The residuals are presented in a separate panel. Introduction of dispersion of k_x as an additional variable produces a much improved fit, as shown by the modified residuals (circles) in Figure 2A. A best-fit dispersion value of $dk_x/d(D-E) = -1.8$ s^{-1}/GHz reduces χ^2 by a factor of 4.6. No significant improvement in χ^2 is obtained for the spectrum of KWK shown in Figure 2B (decreasing frequency) upon introducing $dk_x/d(D-E)$. This response is relatively insensitive to dispersion in k_x, χ^2 exhibiting several shallow minima for $dk_x/d(D-E)$ values between 0 and −2 s^{-1}/GHz. The D−E band of tryptophan with increasing frequency shows a similar reduction in χ^2 with the introduction of dispersion in k_x, but when swept downward it also is fit well with fixed kinetic parameters from MIDP.

The 2E transition of KWK swept in either direction is described well using fixed kinetic parameters from MIDP. On

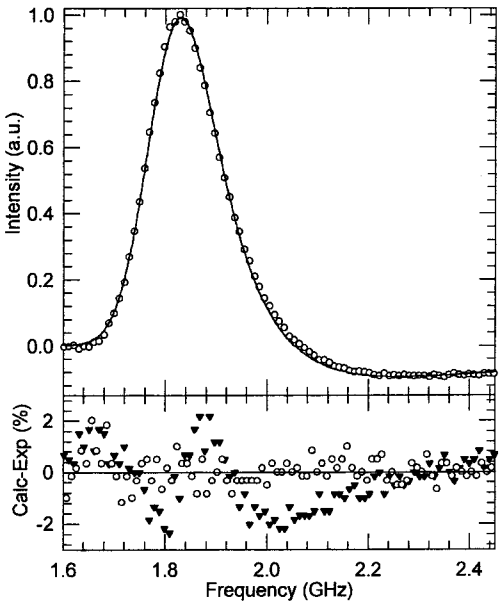

Figure 1. Delayed slow-passage D−E ODMR transition of NATA with microwave frequency increasing at 32 MHz/s (above). Data points (open circles) are plotted for only one-eighth of the recorded data for clarity. The solid line is the least-squares best-fit response calculated with fixed parameters from independent MIDP measurements. The residuals of this fitting are given in the lower panel by filled triangles. Open circles in the lower panel are residuals for best-fit response that incorporates dispersion in k_x.

the other hand, for tryptophan a significantly larger χ^2 is produced for the 2E band with decreasing than with increasing microwave frequency. Introduction of an added dispersion variable, $dk_x/d(2E)$, reduces χ^2 by a factor of 1.8. The best fit value is $+1.0$ s^{-1}/GHz. The D + E ODMR data were fit well for each sample with the fixed parameters obtained from MIDP analysis both with and without EEDOR enhancement. Each ODMR transition of tryptophan and KWK was swept with both increasing and decreasing microwave frequency. The transitions of NATA and RNaseT1 were swept with increasing frequency only.

In Table 1, we compare best-fit values of ν_0, and $\nu_{1/2}$ for each of the samples obtained by the earlier empirical fitting[7] as well as by using fixed input parameters obtained from MIDP, and by introducing dispersion of k_x in the D−E transition. In Table 2, we list the kinetic parameters obtained by global MIDP analysis as well as the best fit dispersion parameters from analysis of the delayed slow passage ODMR spectra.

Discussion

With the exception of RNaseT1 the fitting of delayed slow passage ODMR responses using initial sublevel populations, kinetic, and radiative parameters derived from global analysis of MIDP data sets reveal a systematic deviation in the $T_z \leftrightarrow T_x$ spectrum (D−E transition) with increasing microwave frequency (Figure 1). The quality of fit was improved significantly (Table 1) by introducing dispersion in k_x, the largest of the kinetic parameters (Table 2). Choice of dispersion in this parameter is based on several considerations:

(1) Dispersion in k_z is not possible since $\langle k_z \rangle_{av}$ should be maintained at its MIDP value of zero (Table 2).

(2) Dispersion in k_y is an unlikely cause of the deviation since T_y is not directly involved in the D−E transition, and is only coupled to this transition through small SLR rate constants (Table 2). Also, there is no reason k_y should be correlated with the frequency of a transition that does not involve T_y.

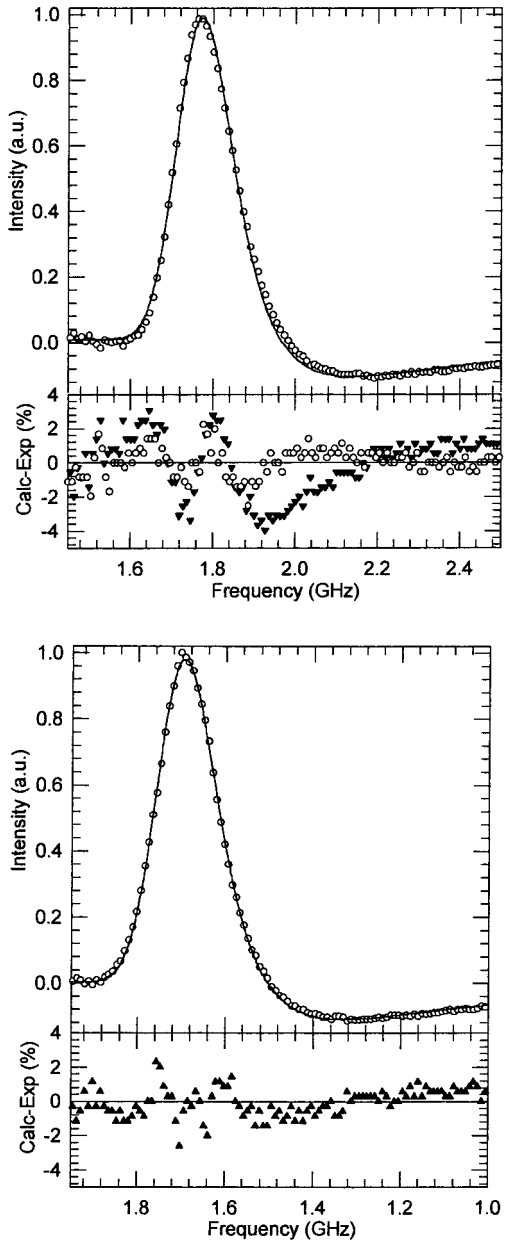

Figure 2. (A, top) The upper panel shows the delayed slow-passage D−E ODMR transition of KWK with microwave frequency increasing at 29 MHz/s. Data points (open circles) are plotted for only one-eighth of the recorded data for clarity. The solid line is the calculated best-fit response using fixed input parameters from independent MIDP measurements. The residuals of this fitting are shown in the lower panel by filled triangles. Open circles in the lower panel are residuals for the best-fit response that incorporates dispersion in k_x. (B, bottom) The upper panel shows the delayed slow-passage D−E ODMR transition of KWK with microwave frequency decreasing at 29 MHz/s. Data points (open circles) are plotted for only one-eighth of the recorded data for clarity. The solid line is the calculated best-fit response using fixed input parameters from independent MIDP measurements. The residuals of this fitting are shown in the lower panel by filled triangles

(3) Attempts to eliminate the deviation by introducing linear dispersion in W_{xz} were made, but χ^2 was found to be insensitive over a reasonable range of values of this parameter.

(4) Other evidence exists that supports dispersion in k_x. In a previous study,[16] k_x was found to vary among a series of nucleic acid complexes of a single tryptophan-containing peptide with widely varying D−E peak frequencies. A correlation between these parameters with $dk_x/d(D-E) = -2.0 \pm 0.5$ s^{-1}/GHz is found. This dispersion has the same sign and the same general

TABLE 1: Band Centers and Widths from Delayed ODMR

sample	method	ν_0 ($\nu_{1/2}$)$_{D-E}$[a]	χ^2[b]	ν_0 ($\nu_{1/2}$)$_{2E}$[a]	χ^2[b]	ν_0 ($\nu_{1/2}$)$_{D+E}$[a]	χ^2[b]
tryptophan	empirical[c]	1.771 (63)	1	2.499 (138)	1	4.249 (94)	1
	MIDP[d]	1.777 (67)	5.36	2.489 (128)	1.22	4.239 (80)	1.14
	MIDP[e]	1.775 (64)	1.64				
KWK	empirical[c]	1.730 (57)	1	2.491 (130)	1		
	MIDP[d]	1.739 (64)	6.77	2.498 (123)	1.34		
	MIDP[e]	1.734 (60)	1.47				
NATA	empirical[c]	1.783 (59)	1	2.463 (129)	1	4.232 (73)[f]	1
	MIDP[d]	1.789 (63)	7.00	2.469 (125)	1.13	4.231 (72)[f]	1.08
	MIDP[e]	1.785 (59)	1.15				
RNAse T_1	empirical[c]	1.753 (38)	1	2.468 (52)	1	g	
	MIDP[d]	1.760 (42)	1.25	2.472 (55)	2.24	g	
	MIDP[e]	1.759 (41)	1.16				

[a] ν_0 is in GHz, and $\nu_{1/2}$ in MHz is in parentheses. Spectra are obtained with increasing microwave frequency. [b] χ^2 is measured relative to χ^2(empirical). See text. [c] Method of ref 7. [d] Fixed kinetic parameters from MIDP, this work. [e] Assuming dispersion in k_x. Best-fit dispersion parameter is given in Table 2. [f] Measured using EEDOR, saturating the 2E transition. [g] Signal quality too poor to analyze.

TABLE 2: Kinetic Parameters for Triplet States

sample	k_x (s^{-1})	k_y (s^{-1})	k_z (s^{-1})	r_{yx}	w_{xy} (s^{-1})	w_{xz} (s^{-1})	w_{yz} (s^{-1})	$dk_x/d(D-E)$[a]	$dk_x/d(2E)$[b]	$\chi^2(2E)$[b]
tryptophan	0.309	0.102	0.00	0.10	0.01	0.04	0.04	−1.1	0[c]	3.30
									+1.0[d]	1.90
KWK	0.331	0.089	0.00	0.07	0.01	0.04	0.04	−1.8	0[c]	1.38
									+0.3[d,e]	1.23
NATA	0.310	0.093	0.01	0.06	0.02	0.03	0.03	−1.2	*f*	
RNAseT1	0.320	0.089	0.01	0.18	0.00	0.07	0.04	−1.6[e]	*f*	

[a] Best-fit value for increasing frequency sweep. χ_{D-E}^2 given in Table 1; units are s^{-1}/GHz. [b] Values are from decreasing frequency sweep; units are s^{-1}/GHz. [c] Fixed value (assumed). [d] Best-fit value. [e] Parameter is of doubtful reliability due to small effect on χ^2. [f] Spectra were not run with decreasing frequency sweep.

magnitude as those determined above for the inhomogeneously broadened populations, greatly supporting the introduction of this variable in the analysis above.

Introducing dispersion in k_x without a corresponding change in the radiative rate constant ratio r_{yx} implies that the dispersion occurs in the nonradiative decay constant, k_x^{nr}. In order to determine whether dispersion in the radiative rate constant is involved, k_x was varied along with a coupled dispersion in the r_{yx} parameter according to

$$dr_{yx}/d(D-E) = -(r_{yx}/\phi_x k_x)_{\nu 0}\, dk_x/d(D-E) \qquad (9)$$

where ϕ_x is the radiative quantum yield of T_x. Equation 9 follows if the dispersion is restricted to k_x^r. From the fluorescence quantum yield, $\Phi_f = 0.72$, and the phosphorescence quantum yield, $\Phi_p = 0.17$, for tryptophan at 77 K[17] along with the sublevel kinetic and radiative parameters of Table 2, it can be concluded that $\phi_x \geq 0.75$. In applying eq 9 we have assumed $\phi_x = 1$ since, if anything, the radiative quantum yields will be larger at 1.2 K than at 77 K. Allowing the associated dispersion in r_{yx} produces no significant improvement in χ^2 and yields the same best fit values for ν_0, $\nu_{1/2}$, and $dk_x/d(D-E)$. It can be concluded that we cannot distinguish between dispersion in the radiative or radiationless part of k_x.

The evidence for correlation of k_x with the frequency of the $T_x \leftrightarrow T_y$ transition (2E band) is rather less compelling. Improvement in χ^2 from the introduction of a variable $dk_x/d(2E)$ is less than that found for the $T_x \leftrightarrow T_z$ transition. Significant improvement is obtained only for the spectrum of tryptophan obtained with decreasing microwave frequency (Table 2), the opposite of that found for the D−E band. Spectra of the 2E band obtained with increasing frequency are fitted well with fixed MIDP parameters in all samples (Table 1). Since the sign of the dispersion is opposite for the 2E and D−E band, it is of interest to note that the introduction of dispersion in k_x only improves the fitting of the spectrum for which the more slowly decaying T_x population is sampled last. The previous study[16] also provides evidence for the correlation of k_x with the frequency of the tryptophan $T_x \leftrightarrow T_y$ transition in a series of peptide−nucleic acid complexes. A weak correlation between these parameters with $dk_x/d(2E) = +1.2 \pm 0.7$ s^{-1}/GHz can be established, but the scattter is large. The positive sign supports the best-fit value found in tryptophan for $dk_x/d(2E)$ in the present work (Table 2).

A linear correlation between the frequency of the D−E ODMR transition and the energy of the phosphorescence 0,0-band of tryptophan ($E_{0,0}$) has been noted for some time.[4,18,19] It has been attributed to solvent perturbations that mix more highly delocalized excited triplet states with the phosphorescent state.[19,20] The value of $d(D-E)/dE_{0,0}$, obtained for a number of tryptophan residues in various environments,[4] is ca. 0.34 MHz/cm^{-1}. In addition, a linear correlation has been observed between k_x and $E_{0,0}$ in a previous study of nucleic acid complexes of a single tryptophan-containing peptide.[16] From this work, we find a value of ca. $-8{\cdot}0 \times 10^{-4}$ s^{-1}/cm^{-1} for $dk_x/dE_{0,0}$. Thus, it is reasonable to find a correlation between k_x and D−E. Using the experimental values above, we would expect to find about -2.3 s^{-1}/GHz for $dk_x/d(D-E)$, a value that is consistent with the delayed slow passage ODMR analyses (Table 2). RNaseT1 appears to be an exception among the tryptophan-containing molecules in this study in that the ODMR bands are fit well with fixed parameters obtained from MIDP. Only a minor improvement in χ^2 is obtained by introducing dispersion in k_x (Table 1). Since this is the only sample in which the tryptophan residue is not solvent exposed, it suggests that the dispersion of k_x may be a consequence of random solvent interactions.

Conclusions

The band shapes of delayed ODMR signals of several tryptophan-containing samples have been analyzed using fixed kinetic, radiative, and sublevel occupancy parameters that were obtained from global analysis of independent MIDP measurements as input. Except for the D−E band ($T_x \leftrightarrow T_z$ transition)

the quality of the fit was satisfactory and comparable to the fitting by a previous empirical method[7] that uses many more variable parameters. This band was fit well by the fixed MIDP parameters only for RNaseT1. The quality of the fit for the D−E band was improved significantly by introducing the dispersion of k_x as an additional fitting parameter. The negative sign and magnitude of the best-fit values of $dk_x/d(D-E)$ are consistent with values predicted from previously observed correlations between kinetic and spectroscopic parameters of the tryptophan triplet state in disordered solids. Positive dispersion of k_x with respect to the 2E frequency is suggested, but only for tryptophan itself. The best-fit values of ν_0 and $\nu_{1/2}$ are changed only slightly in this more rigorous analysis relative to the empirical one, so previously determined frequencies and bandwidths should be considered reliable.

Acknowledgment. This paper was made possible by grant no. ES-02662 from the National Institute of Environmental Health Sciences. Its contents are solely the responsibility of the authors and do not necessarily reflect the official views of the NIEHS, NIH.

References and Notes

(1) Clarke, R. H., Ed.; *Triplet State ODMR Spectroscopy*; Wiley: New York, 1982.
(2) Zuclich, J.; von Schütz, J. U.; Maki, A. H. *J. Am. Chem. Soc.* **1974**, *96*, 710.
(3) Rousslang, K. W.; Ross, J. B. A.; Deranleau, D. A.; Kwiram, A. L. *Biochemistry* **1978**, *17*, 1087.
(4) Hershberger, M. V.; Maki, A. H.; Galley, W. C. *Biochemistry* **1980**, *19*, 2204.
(5) Winscom, C. J.; Maki, A. H. *Chem. Phys. Lett.* **1971**, *12*, 264.
(6) Wu, J. Q.; Ozarowski, A.; Maki, A. H. *J. Magn. Reson. A* **1996**, *119*, 82.
(7) Wu, J. Q.; Ozarowski, A.; Davis, S. K.; Maki, A. H. *J. Phys. Chem.* **1996**, *100*, 11496.
(8) Ozarowski, A.; Wu, J. Q.; Maki, A. H. *J. Magn. Reson. A* **1996**, *121*, 178.
(9) Schmidt, J.; Veeman, W. S.; van der Waals, J. H. *Chem. Phys. Lett.* **1969**, *4*, 341.
(10) Wu, J. Q.; Ozarowski, A.; Maki, A. H. *J. Phys. Chem. A* **1997**, *101*, 6177.
(11) Ozarowski, A.; Wu, J. Q.; Maki, A. H. *Chem. Phys. Lett.* **1998**, *286*, 433.
(12) Kreyszig, E. *Advanced Engineering Mathematics*, 4th ed.; Wiley: New York, 1979; p 359.
(13) Hoff, A. J.; Cornelissen, B. *Mol. Phys.* **1982**, *45*, 413.
(14) Phillips, W. A. *J. Low Temp. Phys.* **1972**, *7*, 351.
(15) Anderson, P. W.; Halperin, B. I.; Varma, C. M. *Philos. Mag.* **1972**, *25*, 1.
(16) Wu, J. Q.; Ozarowski, A.; Maki, A. H.; Urbaneja, M. A.; Henderson, L. E.; Casas-Finet, J. R. *Biochemistry* **1997**, *36*, 12506.
(17) Bishai, F.; Kuntz, E.; Augenstein, L. *Biochim. Biophys. Acta* **1967**, *140*, 381.
(18) von Schütz, J. U.; Zuclich, J.; Maki, A. H. *J. Am. Chem. Soc.* **1974**, *96*, 714.
(19) Kwiram, A. L. In *Triplet State ODMR Spectroscopy*; Clarke, R. H., Ed.; Wiley: New York, 1982; p 427.
(20) van Egmond, J.; Kohler, B. E.; Chan, I. Y. *Chem. Phys. Lett.* **1975**, *34*, 423.